Piezoelectric materials mimic the function of the cochlear sensory epithelium

Takatoshi Inaoka[a,1], Hirofumi Shintaku[b,1], Takayuki Nakagawa[a,2], Satoyuki Kawano[b], Hideaki Ogita[a], Tatsunori Sakamoto[a], Shinji Hamanishi[c], Hiroshi Wada[d], and Juichi Ito[a]

[a]Department of Otolaryngology, Head and Neck Surgery, Graduate School of Medicine, Kyoto University, Kyoto 606-8507, Japan; [b]Department of Mechanical Science and Bioengineering, Graduate School of Engineering Science, Osaka University, Osaka 560-8531, Japan; [c]Department of Mechanical Engineering, Sendai National College of Technology, Miyagi 981-1239, Japan; and [d]Department of Bioengineering and Robotics, Graduate School of Engineering, Tohoku University, Miyagi 980-8579, Japan

Edited by Dale Purves, Duke University Medical Center, Durham, NC, and approved September 13, 2011 (received for review June 25, 2011)

Cochlear hair cells convert sound vibration into electrical potential, and loss of these cells diminishes auditory function. In response to mechanical stimuli, piezoelectric materials generate electricity, suggesting that they could be used in place of hair cells to create an artificial cochlear epithelium. Here, we report that a piezoelectric membrane generated electrical potentials in response to sound stimuli that were able to induce auditory brainstem responses in deafened guinea pigs, indicating its capacity to mimic basilar membrane function. In addition, sound stimuli were transmitted through the external auditory canal to a piezoelectric membrane implanted in the cochlea, inducing it to vibrate. The application of sound to the middle ear ossicle induced voltage output from the implanted piezoelectric membrane. These findings establish the fundamental principles for the development of hearing devices using piezoelectric materials, although there are many problems to be overcome before practical application.

cochlear implant | hearing loss | mechanoelectrical transduction | traveling wave | regeneration

The cochlea is responsible for auditory signal transduction in the auditory system. It responds to sound-induced vibrations and converts these mechanical signals into electrical impulses, which stimulate the auditory primary neurons. The human cochlea operates over a three-decade frequency band from 20 Hz to 20 kHz, covers a 120-dB dynamic range, and can distinguish tones that differ by <0.5% in frequency (1). It is relatively small, occupying a volume of <1 cm^3, and it requires ~14 μW power to function (2).

The mammalian ear is composed of three parts: the outer, middle, and inner ears (Fig. 1*A*) (3). The outer ear collects sound and funnels it through the external auditory canal to the tympanic membrane. The cochlea consists of three compartments: scala vestibuli and scala tympani, which are filled with perilymph fluid, and scala media, which is filled with endolymph fluid (Fig. 1*C*). The scala vestibuli and scala tympani form a continuous duct that opens onto the middle ear through the oval and round windows. The stapes, an ossicle in the middle ear, is directly coupled to the oval window. Sound vibration is transmitted from the ossicles to the cochlear fluids through the oval window as a pressure wave that travels from the base to the apex of the scala vestibuli through the scala tympani and finally to the round window (Fig. 1*B*). The scala media are membranous ducts that are separated from the scala vestibuli by Reissner's membrane and separated from the scala tympani by the basilar membrane. The pressure wave propagated by the vibration of the stapes footplate causes oscillatory motion of the basilar membrane, where the organ of Corti is located. The organ of Corti contains the sensory cells of the auditory system; they are known as hair cells, because tufts of stereocilia protrude from their apical surfaces (Fig. 1*D*). The oscillatory motion of the basilar membrane results in the shear motion of the stereociliary bundle of hair cells, resulting in depolarization of hair cells.

The cochlea amplifies and filters sound vibration by means of structural elements, especially the basilar membrane, and through an energy-dependent active process of fine-tuning that is largely dependent on the function of the outer hair cells. The location of the largest vibration in the basilar membrane depends on the frequency of the traveling wave (Fig. 1*E*) (4, 5). The width, thickness, and stiffness of the basilar membrane vary along the length of the cochlear spiral. Because of this variation in mechanical impedance, high-frequency sounds amplify the motion of the basilar membrane near the base of the cochlea, whereas low-frequency sounds amplify its motion near the apex (Fig. 1*E*). Hair cells within a frequency-specific region are selectively stimulated by basilar membrane vibration according to the traveling wave theory. The mechanical filtering of sound frequency by structural elements of the cochlea allows it to function as a highly sophisticated sensor. Additional details of cochlear macro- and micromechanics can be found in the review by Patuzzi (6).

Both inner and outer hair cells are arranged in four rows along the entire length of the cochlear coil (Fig. 1*D*). The single row of inner hair cells plays a central role in transmission of sound stimuli to the auditory primary neurons, whereas the three rows of outer hair cells amplify and filter sound vibration. The outer hair cells are capable of somatic electromotility driven by the molecular motor protein prestin, which is located in the outer hair cell membrane (7). The electromotility of outer hair cells contributes to the fine-tuning to sound frequency (8–11). The stereocilia also play a role in signal amplification in amphibians. Active hair bundle motions correlated with transduction channel gating resonate with the stimulus and enhance basilar membrane movement. A more detailed description of the mechanisms of cochlear amplification can be found in the review by LeMasurier and Gillespie (12).

Sensorineural hearing loss (SNHL) is a common disability caused by loss of hair cells (13, 14). Most cases of SNHL are irreversible, because mammalian hair cells have a limited capacity for regeneration (15, 16). The loss of outer hair cells diminishes the fine-tuning of the cochlea to sound frequency. The loss of inner hair cells results in profound hearing impairment because of lack of transmission of auditory signals from the cochlea to the central auditory system. At present, therapeutic options for profound SNHL are limited to cochlear implants, which have partially restored the hearing of more than 120,000 patients worldwide (17). A cochlear implant has both external and internal parts. The former includes microphones, speech processors, and transmitters, and the latter includes receivers,

Author contributions: H.S., T.N., S.K., T.S., H.W., and J.I. designed research; T.I., H.S., H.O., and S.H. performed research; H.O., S.H., and H.W. contributed new reagents/analytic tools; T.I., H.S., T.N., S.K., T.S., and S.H. analyzed data; and T.I., H.S., and T.N. wrote the paper.

The authors declare no conflict of interest.

This article is a PNAS Direct Submission.

Freely available online through the PNAS open access option.

[1]T.I. and H.S. contributed equally to this work.

[2]To whom correspondence should be addressed. E-mail: tnakagawa@ent.kuhp.kyoto-u.ac.jp.

This article contains supporting information online at www.pnas.org/lookup/suppl/doi:10.1073/pnas.1110036108/-/DCSupplemental.

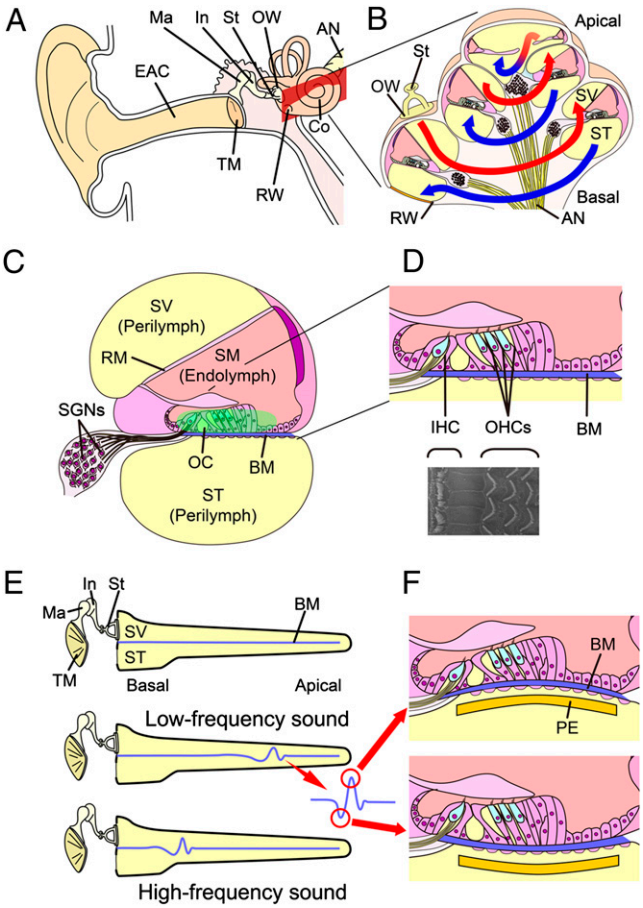

Fig. 1. Anatomy of the mammalian cochlea. (*A*) Schematic drawing of the human auditory system. AN, auditory nerve; Co, cochlea; EAC, external auditory canal; In, incus; Ma, malleus; OW, oval window; RW, round window; St, stapes; TM, tympanic membrane. (*B*) Schematic drawing of a cochlear coil. Sound vibrations transmitted to the cochlea fluid in the scala vestibule (SV) through the OW travel up from the basal turn to the apical turn (red lines) and then back to the basal turn (blue lines) in the scala tympani (ST). (*C*) Schematic drawing of a cochlear duct. The ST and SV are filled with the perilymph. The scala media (SM), which is separated from the ST by Reissner's membrane (RM) and separated from the ST by the basilar membrane (BM), is filled with the endolymph. The organ of Corti (OC) is located on the BM. Spiral ganglion neurons (SGNs) are located in the modiolus of the cochlea. (*D*) Schematic drawing and scanning EM of the organ of Corti. One row of inner hair cells (IHCs) and three rows of outer hair cells (OHCs) are arranged along the entire length of the cochlear coil. (*E*) Schematic drawing of traveling wave theory. Low-frequency sounds vibrate the BM in the apical portion of a cochlea, whereas high-frequency sounds provoke vibration in the basal portion of a cochlea. (*F*) Schematic drawing showing the vibration of the BM and a piezoelectric membrane (PE) implanted in the ST of a cochlea in response to sound stimuli.

stimulators, and electrode arrays, which are surgically inserted under the skin or into the cochlea. Arrays of up to 24 electrodes are generally implanted into the scala tympani, and they directly stimulate the auditory primary neurons. The conversion of sound stimuli to electrical signals is performed by the external speech processor and transmitter and the internal receiver and stimulator. A battery is required to generate electrical output. Schematics and additional descriptions of the history, present status, and future directions of cochlear implants can be found in the work by Zeng et al. (17).

The traveling wave theory proposed by von Békésy (4, 5) was validated using cochleae from cadavers, indicating that, even after complete loss of hair cell function, the mechanical tonotopy for sound frequency remains within the cochlea. This phenomenon also persists in deafened cochleae. However, to our knowledge, electrical hearing devices have not yet used mechanical cochlear tonotopy for sound frequency. In theory, an implantable device that converts sound vibration to electric potential could be fabricated using microelectromechanical systems and implanted close to the basilar membrane of the cochlea. The vibration of the basilar membrane in response to sound stimuli should be transmitted to the implanted device, generating an electrical output (Fig. 1*F*). According to the traveling wave theory, tuning for sound frequency should be determined largely by where the device is implanted.

To test this hypothesis, we developed a prototype artificial cochlear epithelium using a piezoelectric membrane, which functions as a sensor with the capability for acoustic/electric conversion without a battery (18). The piezoelectric device, although not life-sized, showed a tonotopic map for frequencies of 6.6–19.8 kHz in air and 1.4–4.9 kHz in silicone oil, and it generated maximum electrical output from an electrode placed at the site of maximum vibration. In the present study, we showed that the electrical output from a prototype device in response to sound stimuli induced auditory brain-stem responses (ABRs) in deafened guinea pigs. We fabricated a life-sized device using microelectromechanical systems and tested its responses to sound application when implanted in the guinea pig cochlea. Our findings are a major step to developing an implantable artificial cochlear epithelium that can restore hearing.

Results and Discussion

Effects of Kanamycin and Ethacrynic Acid on Auditory Primary Neurons and Hair Cells. To examine the potential of a piezoelectric device to induce biological ABRs in deafened guinea pigs, we established a model in which all hair cells were lost but auditory primary neurons remained to avoid the confounding effects of hair cell-mediated responses. Adult Hartley guinea pigs ($n = 6$) were administered an i.m. injection of kanamycin (KM; 800 mg/kg) followed by an i.v. injection of ethacrynic acid (EA; 80 mg/kg), and the compound action potential was measured to monitor hearing function. A total loss of hearing was observed 7 d after the administration of drugs in all animals at all tested frequencies. We then examined the thresholds of electrically evoked ABRs (eABRs), which are generated by direct electrical stimulation of the auditory primary neurons to determine the survival of these cells in the animal model. Measurements of eABR showed no significant elevation of eABR thresholds in animals treated with KM and EA compared with normal animals (2.50 ± 0.50 V in normal animals, 2.83 ± 0.37 V in test animals). Histological analysis revealed no significant loss of spiral ganglion, whereas there was a total of loss of hair cells in test animals (Fig. S1).

Generation of ABRs by a Piezoelectric Device in Living Guinea Pigs. A prototype piezoelectric device (Fig. 2*A*) containing a PVDF membrane (40-μm thickness) was fabricated using microelectromechanical systems as described previously (18). The piezoelectric membrane was used as a transducer, and its electrical outputs were amplified by 1,000-fold. For stimulation of auditory primary neurons, platinum–iridium ball electrodes were implanted into the scala tympani of the cochlear basal turn (Fig. 2*B*). Typical ABRs in response to increased acoustic stimuli were recorded in our model animals (Fig. 2*C*).

When acoustic stimuli of 104.4 dB sound pressure level (SPL) were applied to the piezoelectric membrane, the first positive wave of ABRs was clearly identified at a latency of 1.07 ± 0.05 ms (Fig. 2*C*), which was identical to the latency of the first positive wave in eABRs (0.98 ± 0.06 ms) in guinea pigs in the present study (Fig. S2). In general, the first wave of eABRs corresponds to wave II of normal ABRs (19). Compared with the latency of wave II of normal ABRs in normal guinea pigs ($n = 4$, 2.99 ± 0.11 ms) (Fig. S2), the latency of the first positive wave of piezoelectric device-induced ABRs was ~2 ms short. However, the latency of the first positive wave of piezoelectric device-

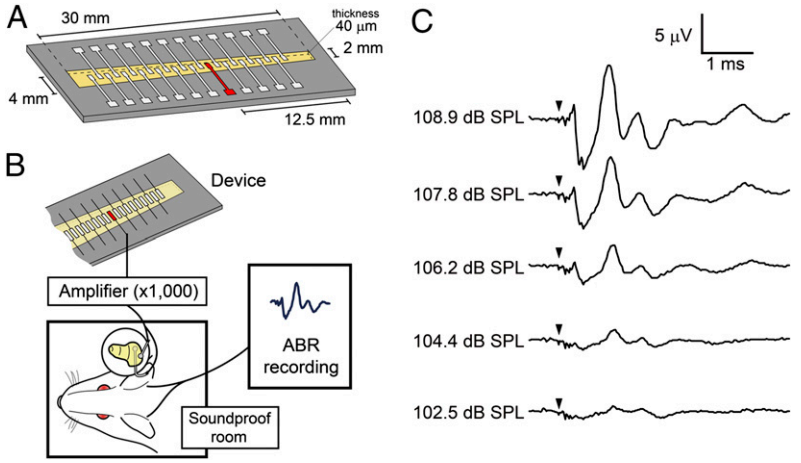

Fig. 2. ABR recording using a prototype device. (*A*) Schematic drawing of a prototype device with a piezoelectric membrane (yellow). A piezoelectric membrane has a thickness of 40 μm and a length of 30 mm. An array of 24 electrodes, made of aluminum thin film, is fabricated on the upper side of a piezoelectric membrane, which is aligned in the midline of the trapezoidal slit of the stainless plate. An electrode used in the experiment of stimulating auditory primary neurons is located 12.5 mm from the shorter side of the trapezoidal membrane (shown in red). (*B*) Schematic drawing of a setting for ABR recording using a piezoelectric device. Electrical signals generated by a piezoelectric membrane in response to acoustic stimuli are amplified and transferred to the cochlea. Bioelectrical signals were recorded as ABRs from needle electrodes inserted dorsal to ears. (*C*) ABRs by electrical signals derived from a prototype device by acoustic stimuli. Arrowheads indicate the timing of acoustic stimuli.

induced ABRs was almost similar to the latency between waves I and II of normal ABRs (0.83 ± 0.04 ms). These findings showed that the piezoelectric membrane generated biological ABRs by converting acoustic stimuli to electrical signals.

Transmission of Sound Vibration from the External Auditory Canal to the Implanted Piezoelectric Device. The transmission of sound waves from the external auditory canal to a piezoelectric membrane implanted into the cochlea is crucial to realize hearing recovery by a piezoelectric device based on the traveling wave theory. To test the transmission of sound waves from the external auditory canal to a piezoelectric membrane, we developed an implantable device that was specialized for the basal turn of the guinea pig cochlea (Fig. 3 *A* and *B*). The device contained a PVDF fluoride trifluoroethylene [P(VDF-TrFE)] membrane with a frequency response of 16–32 kHz, which corresponded to

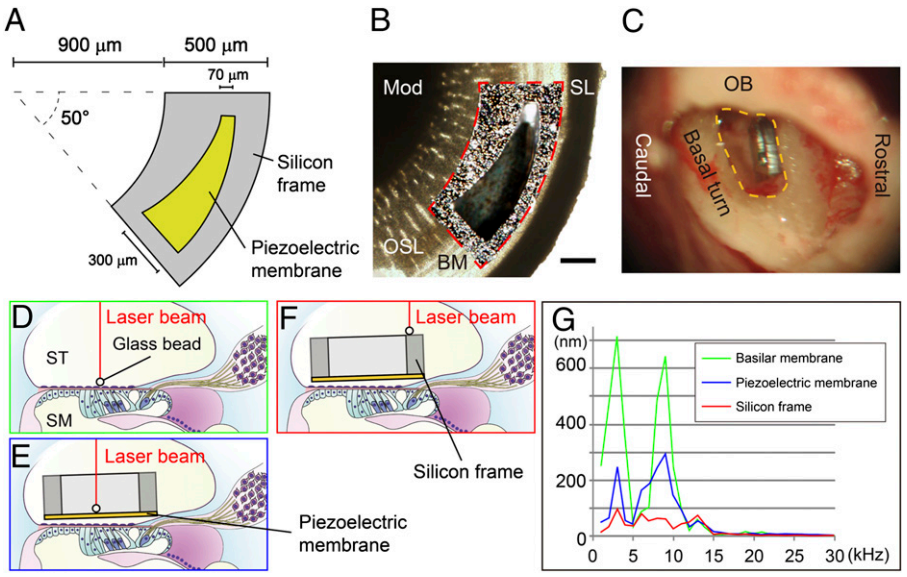

Fig. 3. Sound transmission from the external auditory canal to a piezoelectric device implanted in the cochlea. (*A*) Design of an implantable piezoelectric device. (*B*) A merged image of an implantable piezoelectric device and the basal turn of the guinea pig cochlea. To determine the radius of curvature of the outer border and the inner border of the fan-shaped silicon frame and location of the slit in the silicon frame, we measured radius of curvature of the cochlear basal turn, length between an inner edge of the spiral ligament (SL) and a medial end of the osseous lamina (OSL) where the device will be implanted, and length of the basilar membrane (BM; length between inner edge of spiral ligament and lateral end of osseous lamina). An outline of the silicon frame is shown by a red dotted line. The silicon frame is positioned on the osseous spiral lamina, and the slit of the device is located adjacent to the BM. Mod, cochlear modiolus. (Scale bar: 200 μm.) (*C*) A microscopic view of an implanted device in the basal turn of the guinea pig cochlea. The yellow dotted line indicates an opening in the basal turn of the cochlea. OB, otic bulla. (*D–F*) Schematic drawings of measuring vibration amplitudes using a laser Doppler vibrometer. A glass bead is placed on the BM (*D*), piezoelectric membrane (*E*), or silicon frame (*F*). Red lines indicate a laser beam from a laser Doppler vibrometer. SM, scala media; ST, scala tympani. (*G*) Vibration amplitudes of a BM (green), piezoelectric membrane (blue), and silicon frame (red) corresponding to frequencies of applied sounds.

the response of the basal turn of guinea pig cochleae (20). We implanted the device into the scala tympani of the basal portion of an intact cochlea (Fig. 3*C*). Before implantation, we measured the vibration of the basilar membrane in response to sound stimuli from the external auditory canal at various frequencies between 1 and 30 kHz. A glass bead (50-μm diameter) was placed on the basilar membrane (Fig. 3*D*), and its movement was measured using a laser Doppler vibrometer (21). When continuous pure tones were applied through the external auditory canal, the amplitudes for vibration of the basilar membrane showed peaks at 3 and 9 kHz (Fig. 3*G*, green line). In response to 3 kHz sound stimuli at 101.7 dB SPL, the largest amplitude was 642 nm, which was consistent with previous observations (21). Measurements of the vibratory movements of the piezoelectric membrane (Fig. 3*E*) also revealed two peaks of vibration amplitudes similar to the peaks of the basilar membrane (Fig. 3*G*, blue line). The maximum amplitude of the piezoelectric membrane was 293 nm in response to 9 kHz sound stimuli at 109.2 dB SPL.

In contrast to the piezoelectric membrane, measurements of the movements of the silicon frame (Fig. 3*F*) revealed no apparent peaks in the amplitudes of oscillations, which were all within 100 nm (Fig. 3*G*, red line). The differences in response between the piezoelectric membrane and silicon frame may be caused by the difference in the stiffness. In addition, the piezoelectric membrane was located closer to the basilar membrane than the silicon frame, and the basilar membrane may be a preferable location to receive sound vibration. These findings showed that sound stimuli transmitted through the external auditory canal caused vibration of a piezoelectric membrane implanted within the scala tympani of cochleae. Notably, the piezoelectric membrane exhibited similar tuning for sound frequency as the basilar membrane, indicating that it could reproduce the mechanical tonotopy of the latter. The tuning for sound frequency of the basilar and piezoelectric membranes differed from the tuning of the basilar membrane in normal guinea pig cochleae, which might have been caused by the opening of the cochlear wall for implantation of the device and taking measurements using a laser Doppler vibrometer.

Generation of Voltage Output by the Implanted Device in Response to Sound Stimuli. To show the technical feasibility of the piezoelectric hearing device, we examined whether sound stimuli generated electrical output from the piezoelectric membrane after implantation into the cochlea. For this purpose, we established an ex vivo model of a guinea pig temporal bone, in which sound stimuli were directly applied to the stapes, which transmits sound vibration to the oval window of the cochlea (Fig. 1 *A* and *B*). A miniaturized device modified to contain a silicon rod carrying electrodes for monitoring the voltage output from the piezoelectric membrane (Fig. 4 *A* and *B*) was implanted into the basal portion of cochleae. A miniaturized device was able to generate electrical output ranging from 0.14 to 5.88 mV in response to sound stimuli at 100 dB SPL at frequencies of 1–40 kHz in air (Fig. S3).

When 30-cycle tone-burst stimuli at 100 dB SPL at a frequency of 5, 10, or 20 kHz were directly applied to the stapes using an actuator, peak to peak voltage output of 23.7, 5.7, or 29.3 μV was recorded, respectively (Fig. 4*C*). After completion of the sound application, the amplitudes of voltage output gradually decreased and returned to the original level within 3 ms, which mimicked the biological response of the basilar membrane. In a control setting, in which an actuator generated sound stimuli but was not attached to the stapes, negligible voltage output was recorded (Fig. 4*C*). These findings showed that sound stimuli from the stapes generated voltage output from the piezoelectric device implanted in the cochlea. Notably, the voltage outputs from the piezoelectric device differed depending on the applied

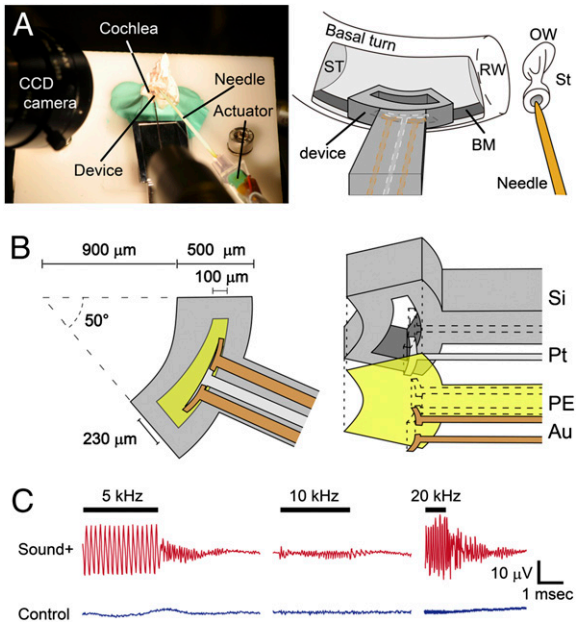

Fig. 4. Electrical output from the piezoelectric membrane implanted in the guinea pig cochlea in response to sound application to the stapes. (*A*) Photograph and schematic drawing showing the setting of an ex vivo system. A guinea pig temporal bone was set on a stage, and an implantable device was inserted into the scala tympani (ST) of the basal turn and placed close to the basilar membrane (BM). A needle was attached on the head of the stapes (St) to transmit sound vibrations through the oval window (OW). RW, round window. (*B*) Design of the implantable piezoelectric device. Au, gold film electrode; PE, piezoelectric membrane; Pt, platinum film electrode; Si, silicon frame. (*C*) Electrical output from a piezoelectric membrane in response to sound stimuli. Bars indicate the period for sound application. Waveforms in red show electrical output when sound stimuli are applied to the stapes, and waveforms in blue show those in a control setting.

sound frequency. The maximum voltage outputs in response to 5 and 20 kHz sound stimuli were similar (23.7 and 29.3 μV, respectively), whereas the outputs in response to 10 kHz sound stimuli were smaller (5.7 μV).

Researchers have previously attempted to develop an artificial cochlea that functions as a highly sophisticated sensor. Studies by von Békésy (4, 5) showing traveling waves in the basilar membrane using cochleae from cadavers led to the development of several physical models of the cochlea. The first group of these models comprised scaled-up versions of the cochlea (22–24). Recently, researchers have developed fluid-filled microscale models that respond to sound in a manner similar to the mammalian cochlea. The work by Zhou et al. (25) showed a tonotopic map over the 0.3- to 15-kHz band in a life-sized model. The work by Chen et al. (26) developed a beam array fixed on a trapezoidal channel and investigated the vibrating characteristics in water. The work by Wittbrodt et al. (27) developed a device containing a polyimide membrane with an aluminum frame, which shared some similarities with the biological cochlea in terms of traveling waves. The work by White and Grosh (28) used silicon micromachining technology to create their cochlea model. This work was important, because the batch micromachining process used to fabricate this system paved the way for the future integration of sensing elements into the structure to produce low-power, micromechanical, and cochlear-type sensor filters. However, these devices have no potential for generating electrical output in response to sound stimuli. Providing high-quality hearing through the cochlear implant involves the development of a device with high channel capability, low-power requirements, and small size (29). The work by Bachman et al. (29) fabricated

a micromechanical multiband transducer that consisted of an array of micromachined polymer resonators, and it examined its sensitivity to sound frequency; however, the work focused on the low-power requirements of the transducer and proposed a design that could be implanted into the middle ear cavity (29), which fundamentally differed from our concept.

The present report describes a device at the technology–biology interface that can mimic the function of the basilar membrane and inner hair cells using a combination of traditional traveling wave theory and microelectromechanical systems. This device could be described as the technological regeneration of hair cells. The device, which consists of a piezoelectric membrane and silicon frame, can be implanted into the guinea pig cochlea. It is able to resonate in response to sound stimuli similar to the natural basilar membrane and generate electric output, whereas previously reported devices required an electrical supply, and realizing low-energy requirements remains a goal for the future development of cochlear implants (29). We, therefore, consider the ability of our device to generate electrical output in response to sound stimuli to be a great advantage. In practice, the electrical output from our device is not sufficient to stimulate auditory primary neurons. The electrical output should be 10^5-fold higher than the output of the present device for effective stimulation of auditory primary neurons when electrodes are placed in the scala tympani similar to conventional cochlear implants. We should optimize the location and fixation of a piezoelectric device in a cochlea for obtaining the maximum oscillation of a piezoelectric membrane, because electrical output from a piezoelectric membrane after implantation in a cochlea decreased to ~10% of electrical output recorded in the in vitro setting (Fig. S3). To increase the power of a piezoelectric device, we will examine the potential of other piezoelectric materials for generation of electrical output and the effects of reduction in thickness of a piezoelectric membrane and multilayer constructions of piezoelectric membranes. In addition, it is also important to reduce electrical output required for sufficient stimulation of auditory primary neurons. For this purpose, we are developing microelectrodes that are able to access close to auditory primary neurons. Finally, our device has only passive sensitivity to sound frequencies. To enhance this sensitivity, additional mechanisms mimicking the function of outer hair cells need to be developed.

Materials and Methods

Experimental Animals. A total of 26 female adult Hartley guinea pigs (4–10 wk, 300–600 g in weight; Japan SLC) with a normal Preyer pinna reflex served as the experimental animals. Animal care was conducted under the supervision of the Institute of Laboratory Animals, Graduate School of Medicine, Kyoto University, Japan. All experimental procedures followed the National Institutes of Health Guidelines for the Care and Use of Laboratory Animals. In all procedures necessitating general anesthesia, the animals were administered an i.m. injection of midazolam (10 mg/kg; Astellas Pharma) and xylazine (0.01 mg/kg; Bayer). Supplemental doses were administered every 2 h or more often if the animal withdrew its leg in response to applied pressure.

eABR Recording. Measurements of eABRs were performed as previously described (30). Biphasic voltage pulses were generated under computer control using a real-time processor (Tucker-Davis Technologies). Electrical stimuli were applied between two intracochlear platinum–iridium electrodes. Bioelectrical signals were digitally amplified, averaged for 500 repetitions, and recorded using subdermal stainless steel needle electrodes.

Prototype Piezoelectric Device. The prototype piezoelectric device was fabricated as previously described (18). A thin aluminum film was formed on both sides of the 40-μm-thick PVDF membrane by sputtering. An electrode array with 24 rectangular elements was fabricated from the aluminum film using a standard photolithography and etching process on the upper side of the PVDF membrane. The aluminum film on the lower side served as a ground electrode.

Prototype Device ABRs. The ABRs produced using the prototype device were measured 7 d after the administration of KM and EA. The generation of trigger signals and the recordings of the evoked potentials were performed using PowerLab/4sp. The trigger signals were conveyed to a function generator (WF1945B; NF Corporation), which was programmed to generate a sinusoidal output signal for each trigger. The amplitudes and frequencies of the sinusoidal outputs were digitally controlled at a base frequency and duration of 5 kHz and 0.2 ms, respectively. The output signals were connected to a custom-made actuator, which delivered acoustic waves to the device. The amplitudes applied to the actuator were calibrated to produce vibrations of the piezoelectric membrane of the device equivalent to those vibrations produced by the application of sound at pressure levels ranging from 87 to 115 dB SPL. The electrical signals generated by the prototype device in response to the acoustic waves of the actuator were transmitted to a custom-made amplifier, which produced a 1,000-fold increase, and their waveforms and amplitudes were monitored by an oscilloscope (WaveJet 314A; LeCroy). A biphasic signal was extracted from the electrical signals using a custom-made complementary metal oxide semiconductor switch to prevent the signal induced by reverberation of the piezoelectric membrane. Signals from the complementary metal oxide semiconductor switch were also conducted to platinum–iridium electrodes implanted in the scala tympani of the cochlear basal turn of guinea pigs (n = 4) placed in a soundproof room. The bioelectrical signals were averaged for 500 repetitions, and they were recorded using subdermal stainless steel needle electrodes. The responses were verified at least two times.

Implantable Miniaturized Device. An implantable device for examining the transmission of sound from the external auditory canal to the piezoelectric membrane was fabricated using a P(VDF-TrFE) membrane (KF-W#2200; Kureha) and a silicon frame according to the methods described previously (31). The surface of the 300-μm-thick silicon substrate (100) was penetrated by hexamethyldisilazane (Tokyo Ohka Kogyo) to enhance adhesion of the P(VDF-TrFE) membrane. An *N*,*N*-dimethylformamide (Nacalai Tesque) solution containing P(VDF-TrFE) at a concentration of 8% weight was spun on the silicon substrate. It was then heated to crystallize the P(VDF-TrFE) at a thickness of 3 μm. The opposite side of the silicon substrate was treated with photolithography and an etching process to form a fan-shaped silicon frame with a slit to accommodate the flexible piezoelectric membrane. The fan-shaped silicon frame and the location of the slit were designed based on the shape of the cochlear basal turn of adult guinea pigs. The slit in the silicon frame was positioned such that the sheet was adjacent to the portions of the basilar membrane where it vibrated the most (32).

Surgical Procedure for Implantation of the Miniaturized Device into the Cochlea. A laser Doppler vibrometer (LV-1100; Ono Sokki) was used to measure the vibrations of the basilar membrane and the piezoelectric membrane of the device implanted in the cochlea. Under general anesthesia, a retroauricular incision was made to expose the bulla of an experimental animal with a normal cochlea (n = 1). An opening was made in the otic bulla while preserving the tympanic annulus, tympanic membrane, and ossicles. This opening was used to direct the laser beam to the cochlea to measure the vibrations. After a skin incision in the submandibular region, cochleostomy was made in the scala tympani of the basal turn for insertion of the implantable device. After a tracheotomy, suxamethonium chloride hydrate (10 mg; Kyorin Pharmaceutical) was injected i.m., and a ventilation tube was inserted into the trachea to suppress movements from spontaneous ventilation.

Measurement of Vibrations Using a Laser Doppler Vibrometer. Sine wave signals produced by a function generator were delivered to an electrostatic speaker driver (ED1; Tucker-Davis Technologies) to generate pure tones from an electrostatic speaker as acoustic stimuli. Continuous pure tones were applied through the external auditory canal of the animals from 1 to 30 kHz at 1-kHz intervals at levels between 62.5 and 109.2 dB SPL. We measured the vibrations in response to sound stimuli using a laser Doppler vibrometer (21, 33). Initially, a glass bead (50-μm diameter) was set on the basilar membrane. A laser Doppler vibrometer beam was directed to the glass bead (Fig. 3). The vibrations of the basilar membrane were measured five times for each frequency and averaged using a custom-made program. Subsequently, the miniaturized device was manually inserted into the scala tympani with its piezoelectric membrane adjacent to the basilar membrane. The laser beam was directed to a glass bead either placed on the surface of the piezoelectric membrane (Fig. 3) or fixed on the silicon frame (Fig. 3) of the implantable device for reflection to detect vibrations.

Miniaturized Device for Voltage Output Recording. The design of an implantable miniaturized device for vibration measurement was modified to record the voltage output from the piezoelectric membrane after implan-

tation into a cochlea. An implantable miniaturized device was connected to a silicon rod carrying electrodes for monitoring the voltage output from the piezoelectric membrane. Two thin (40-nm thickness) gold electrodes, which faced the basilar membrane of the cochlea, were formed by thermal deposition on the piezoelectric membrane. One thin (100-nm thickness) platinum electrode was formed by rf magnetron sputtering on the opposite side of the piezoelectric membrane for recording the output voltage.

Recording Voltage Output from the Piezoelectric Membrane in Response to Sound Stimuli. Two right temporal bones of guinea pigs were used. The bony wall of the otic bulla was removed to expose the basal portion of the cochleae and the incudostapedial joint. After separating the head of the stapes from the incus, the tympanic membrane, malleus, and incus were removed. Cochleostomy of the basal portion of cochleae was performed to access the scala tympani. The temporal bones were then fixed on a stage. The head of the stapes and an actuator (AE0203D04F; NEC/TOKIN) were connected with a needle. The position of the tip of the needle was monitored by a CCD camera during the recording. Tone-burst signals were delivered to an actuator using a function generator (NF Corporation). A modified miniaturized device was inserted into the scala tympani of the basal portion of the cochleae through the cochleostomy site, and it was attached to the piezoelectric membrane and the basilar membrane using a micromanipulator. The scala tympani was filled with 285 mM mannitol solution during the recording. The voltage outputs from the piezoelectric membrane were transmitted to a custom-made amplifier that produced a 1,000-fold increase, and their waveforms and amplitudes were monitored with an oscilloscope (WaveRunner 44MXi-A; LeCroy).

ACKNOWLEDGMENTS. The authors thank Shin-ichiro Kitajiri and Norio Yamamoto for technical contributions to histological analyses and Kozo Kumakawa, Yasushi Naito, and Harukazu Hiraumi for contributions to the development of surgical procedures. This study was supported by grants for Research on Sensory and Communicative Disorders from the Japanese Ministry of Health, Labor and Welfare (to J.I.).

1. Dallos P (1996) *The Cochlea*, eds Dallos P, Popper AN, Fay RR (Springer, New York), pp 1–43.
2. Sarpeshkar R, Lyon RF, Mead C (1998) A low-power wide-dynamic-range analog VLSI cochlea. *Analog Integr Circuits Signal Process* 16:245–274.
3. Slepecky NB (1996) *The Cochlea*, eds Dallos P, Popper AN, Fay RR (Springer, New York), pp 44–129.
4. von Békésy G (1960) *Experiments in Hearing*, ed Wever EG (McGraw-Hill, New York), pp 404–429.
5. von Békésy G (1970) Travelling waves as frequency analysers in the cochlea. *Nature* 225:1207–1209.
6. Patuzzi R (1996) *The Cochlea*, eds Dallos P, Popper AN, Fay RR (Springer, New York), pp 186–257.
7. Belyantseva IA, Adler HJ, Curi R, Frolenkov GI, Kachar B (2000) Expression and localization of prestin and the sugar transporter GLUT-5 during development of electromotility in cochlear outer hair cells. *J Neurosci* 20:RC116.
8. Davis H (1983) An active process in cochlear mechanics. *Hear Res* 9:79–90.
9. Evans BN, Dallos P (1993) Stereocilia displacement induced somatic motility of cochlear outer hair cells. *Proc Natl Acad Sci USA* 90:8347–8351.
10. Zheng J, et al. (2000) Prestin is the motor protein of cochlear outer hair cells. *Nature* 405:149–155.
11. Liberman MC, et al. (2002) Prestin is required for electromotility of the outer hair cell and for the cochlear amplifier. *Nature* 419:300–304.
12. LeMasurier M, Gillespie PG (2005) Hair-cell mechanotransduction and cochlear amplification. *Neuron* 48:403–415.
13. Liberman MC, Rosowski JJ, Lewis RF (2010) *Schuknecht's Pathology of the Ear*, eds Merchant SN, Nadol JB (People's Medical Publishing House-USA, Shelton, CT), 3rd Ed, pp 104–127.
14. Merchant SN (2010) *Schuknecht's Pathology of the Ear*, eds Merchant SN, Nadol JB (People's Medical Publishing House-USA, Shelton, CT), 3rd Ed, pp 631–663.
15. Diaz RC (2009) Inner ear protection and regeneration: A 'historical' perspective. *Curr Opin Otolaryngol Head Neck Surg* 17:363–372.
16. Oshima K, Suchert S, Blevins NH, Heller S (2010) Curing hearing loss: Patient expectations, health care practitioners, and basic science. *J Commun Disord* 43:311–318.
17. Zeng FG, Rebscher S, Harrison WV, Sun X, Feng H (2008) Cochlear implants: System design, integration and evaluation. *IEEE Rev Biomed Eng* 1:115–142.
18. Shintaku H, et al. (2010) Development of piezoelectric acoustic sensor with frequency selectivity for artificial cochlea. *Sens Actuators A* 158:183–192.
19. Yamane H, Marsh RR, Potsic WP (1981) Brain stem response evoked by electrical stimulation of the round window of the guinea pig. *Otolaryngol Head Neck Surg* 89: 117–124.
20. Viberg A, Canlon B (2004) The guide to plotting a cochleogram. *Hear Res* 197:1–10.
21. Wada H, Homma Y, Takahashi S, Takasaka T, Ohyama K (1996) *Proceedings of the International Symposium on Diversity in Auditory Mechanics*, eds Lewis ER, et al. (World Scientific, Teaneck, NJ), pp 284–290.
22. Helle R (1977) Investigation of the vibrational processes in the inner ear with the aid of hydromechanical models. *J Audiol Techn* 16:138–163.
23. Chadwick RS, Fourney ME, Neiswander P (1980) Modes and waves in a cochlear model. *Hear Res* 2:475–483.
24. Lechner TP (1993) A hydromechanical model of the cochlea with nonlinear feedback using PVF2 bending transducers. *Hear Res* 66:202–212.
25. Zhou G, Bintz L, Anderson DZ, Bright KE (1993) A life-sized physical model of the human cochlea with optical holographic readout. *J Acoust Soc Am* 93:1516–1523.
26. Chen F, et al. (2006) A hydromechanical biomimetic cochlea: Experiments and models. *J Acoust Soc Am* 119:394–405.
27. Wittbrodt MJ, Steele CR, Puria S (2006) Developing a physical model of the human cochlea using micro-fabrication methods. *Audiol Neurootol* 11:104–112.
28. White RD, Grosh K (2005) Microengineered hydromechanical cochlear model. *Proc Natl Acad Sci USA* 102:1296–1301.
29. Bachman M, Zeng FG, Xu T, Li GP (2006) Micromechanical resonator array for an implantable bionic ear. *Audiol Neurootol* 11:95–103.
30. Ogita H, et al. (2009) Surgical invasiveness of cell transplantation into the guinea pig cochlear modiolus. *ORL J Otorhinolaryngol Relat Spec* 71:32–39.
31. Shintaku H, et al. (2010) Culturing neurons on MEMS fabricated P(VDF-TrFE) films for implantable artificial cochlea. *J Biomech Sci Eng* 5:229–235.
32. Nilsen KE, Russell IJ (1999) Timing of cochlear feedback: Spatial and temporal representation of a tone across the basilar membrane. *Nat Neurosci* 2:642–648.
33. Wada H, et al. (1999) Measurement of dynamic frequency characteristics of guinea pig middle ear by a laser Doppler velocimeter. *JSME Int J Ser C* 42:753–758.